tvst

DOI: 10.1167/tvst.6.4.6

Article

Progression of Local Glaucomatous Damage Near Fixation as Seen with Adaptive Optics Imaging

Donald C. Hood[1,2], Dongwon Lee[1], Ravivarn Jarukasetphon[3], Jason Nunez[1], Maria A. Mavrommatis[1], Richard B. Rosen[3], Robert Ritch[3], Alfredo Dubra[4], and Toco Y. P. Chui[3]

[1] Department of Psychology, Columbia University, New York, NY, USA
[2] Department of Ophthalmology, Columbia University, New York, NY, USA
[3] New York Eye & Ear Infirmary of Mount Sinai, New York, NY, USA
[4] The Eye Institute, Medical College of Wisconsin, Milwaukee, WI, USA

Correspondence: Donald C. Hood, Department of Psychology, 406 Schermerhorn Hall, 1190 Amsterdam Ave., MC5501. e-mail: dch3@columbia.edu

Received: 04 March 2017
Accepted: 30 May 2017
Published: 12 July 2017

Keywords: adaptive optics; glaucoma; retinal nerve fiber

Citation: Hood DC, Lee D, Jarukasetpho R, Nunez J, Mavrommatis MA, Rosen RB, Ritch R, Dubra A, Chui TYP. Progression of local glaucomatous damage near fixation as seen with adaptive optics imaging. Trans Vis Sci Tech. 2017;6(4):6, doi: 10.1167/tvst.6.4.6

Purpose: Deep glaucomatous defects near fixation were followed over time with an adaptive optics-scanning light ophthalmoscope (AO-SLO) to better understand the progression of these defects and to explore the use of AO-SLO in detecting them.

Methods: Six eyes of 5 patients were imaged with an AO-SLO from 2 to 4 times for a range of 14.6 to 33.6 months. All eyes had open-angle glaucoma with deep defects in the superior visual field (VF) near fixation as defined by 10-2 VFs with 5 or more points less than −15 dB; two of the eyes had deep defects in the inferior VF as well. AO-SLO images were obtained around the temporal edge of the disc.

Results: In 4 of the 6 eyes, the edge of the inferior-temporal disc region of the retinal nerve fiber (RNF) defect seen on AO-SLO moved closer to fixation within 10.6 to 14.7 months. In 4 eyes, RNF bundles in the affected region appeared to lose contrast and/or disappear.

Conclusions: Progressive changes in RNF bundles associated with deep defects on 10-2 VFs can be seen within about 1 year with AO-SLO imaging. These changes are well below the spatial resolution of the 10-2 VF. On the other hand, subtle thinning of regions with RNF bundles is not easy to see with current AO-SLO technology, and may be better followed with OCT.

Translational Relevance: AO-SLO imaging may be useful in clinical trials designed to see very small changes in deep defects.

Introduction

For well over 20 years, studies have suggested that the macula (i.e., the central ±8° from fixation) can be damaged in early glaucoma.[1–5] However, until recently it generally was assumed by clinicians to be relatively uncommon. Witness, for example, the general use in the clinic of a 24-2 (6° grid) visual field (VF), which poorly samples the macula region[6] and which can miss and/or underestimate the extent of damage.[5–14] However, recent work with optical coherence tomography (OCT) has documented that macular damage is very common early in the glaucomatous process.[6,15,16] In addition, we now have an anatomic explanation for local defects often seen in the superior VF near fixation when patients are tested with a 10-2 (2° grid) VF pattern. In particular, axons of retinal ganglion cells (RGCs) situated in the retinal region just inferior to fixation enter the optic disc in the temporal portion of the inferior quadrant, the quadrant particularly vulnerable to macula damage.[6,8,15] Thus, it is not surprising that early glaucomatous defects often are seen near fixation in the superior visual field.

Because the macula is essential for everyday visual tasks, such as reading and driving,[17,18] it is important to understand the nature of the damage to the macula, especially the deep local defects near fixation. We previously studied eyes with deep defects near fixation as seen on 10-2 VFs with adaptive optics-scanning light ophthalmoscope (AO-SLO) and OCT

Table 1. Time in Months between First and Subsequent AO-SLO Imaging Sessions

		Time between First and Subsequent Visits, mos		
Patient	Eye	Second Visit	Third Visit	Fourth Visit
P1	OS	14.7	30.0	
P2	OD	14.6		
P3OD	OD	17.3	22.8	33.6
P3OS	OS	4.9	15.5	
P5	OS	26.5		
P6	OS	19.1	27.4	

imaging of the circumpapillary region. AO-SLO images have better transverse resolution than do OCT scans, allowing for visualization of the individual retinal nerve fiber (RNF) bundles in healthy and glaucomatous eyes.[19–25] We found that eyes with relatively similar 10-2 defects and similar circumpapillary RNF layer thickness profiles on OCT disc scans had different degrees and patterns of RNF bundle damage as seen on AO-SLO.[25] We examined the progression of this damage in the RNF bundles with AO-SLO. In particular, the purpose here was 2-fold. First, using AO-SLO imaging, we examined the change (progress) over time of these deep defects near fixation, and second, we explored in general the use of the AO-SLO in following these changes over time.

Methods

Subjects

Five of the six patients with glaucoma were tested with AO-SLO as part of a previous study,[25] and they agreed to return for one to three additional AO-SLO imaging sessions. The identifiers (e.g., P1, P2, and so forth) in the present study represent the same patients in the earlier study. For patient P3, both eyes were followed. The times between the first and subsequent AO-SLO sessions are shown in Table 1.

Eyes were selected from a group of 10 eyes with AO-SLO based upon 10-2 VF defects. We were interested in eyes with deep arcuate defects near fixation. All six eyes had deep arcuate defects on the total deviation plot of the 10-2 VF (Humphrey VF Analyzer; Carl Zeiss Meditec, Inc., Dublin, CA), as defined by at least five test points with total deviation values ≤−15 dB on their total deviation plots. Figure 1 shows the 10-2 VF total deviation plots for all six eyes; the values less than −15 dB are enclosed within the red boundaries. To compare the pattern of defects across eyes, the associated probability plots are presented as right eyes in

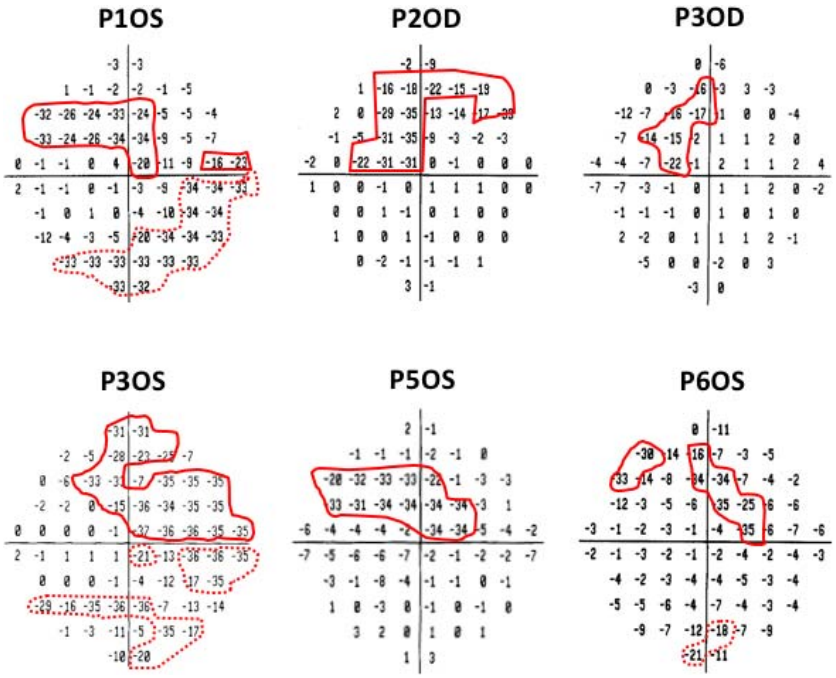

Figure 1. 10-2 visual field total deviation plots. The points close to fixation with total deviation values ≤−15dB are enclosed within the *red borders* in the upper (*solid*) and lower (*dashed*) hemifields.

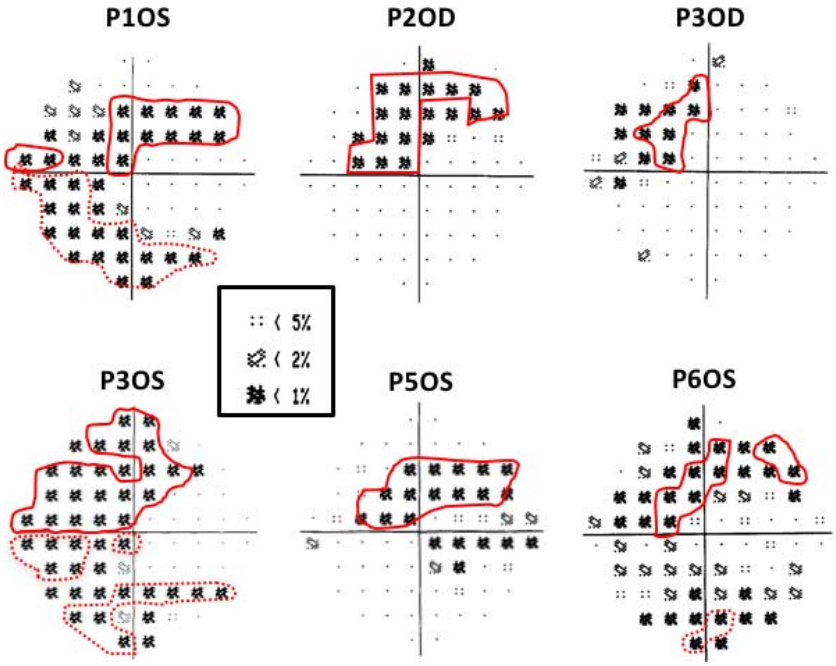

Figure 2. The probability plots for the total deviations plots in Figure 1. All eyes are shown in right eye orientation.

Figure 2 (i.e., left eyes were flipped along the vertical meridian). All six deep defects were within 3° of fixation. In fact, in four of these eyes, the defect included the test point closest to fixation at the right (1°, −1°) and left (1°,1°) eyes. These 10-2 VFs were obtained on the same day as the first AO-SLO session for patients P3OS and P5, and within 3 weeks (patient P1), 9 weeks (patient P2), 4 days (patient P3OD), 7 months (patient P4), and 9 weeks (patient P6) for the other eyes.

Inclusion criteria for AO-SLO imaging were best-corrected visual acuity better than 20/40, clear media, refractive error within ±4.0 D, and pupil dilation ≥6 mm. Patients with intraocular lens implants were excluded. All patients were on intraocular pressure (IOP) lowering medication and there was no reason to suspect they were not compliant. In addition, two eyes had laser treatment during the follow-up period. Patient P1 had selective laser (SLT) and argon laser (ATL) trabeculoplasty between AO-SLO sessions two and three, and patient P3OD had SLT between AO-SLO sessions 1 and 2. Table 2 contains the diagnosis, age at the first AO-SLO session, IOP at each AO-SLO session, range of IOP over all intervening visits, and systemic and ocular comorbidities.

Written, informed consent was obtained from all participants. Procedures followed the tenets of the Declaration of Helsinki, and the protocol was approved by the institutional review boards of

Table 2. Diagnosis, Age at First AO-SLO Session, IOP and Comorbidity Information

Patient	Eye	Dx	Age, First Visit	IOP, d of AO	IOP, range	Systemic and Ocular Comorbidities
P1	OS	PG	59.2	13,15,10	10–18	OSA on CPAP; hypothyroid
P2	OD	OAG	53.4	16,19	15–19	Disc hemorrhage 8 y before to first AO-SLO session
P3OD	OD	OAG	43.3	14,23,20,18	14–23	Ocular surface disease associated with glaucoma medications
P3OS	OS	OAG	43.3	17,18,15	12–19	Ocular surface disease associated with glaucoma medications
P5	OS	NTG	65.9	19,13	11–19	Migraines
P6	OS	OAG	63.2	14,26,20	12–20	OSA on CPAP

CPAP, continuous positive airway pressure; NTG, normal tension glaucoma; OAG, open angle glaucoma; OSA, obstructive sleep apnea; PG, pigmentary glaucoma.

Columbia University and the New York Eye and Ear Infirmary of Mount Sinai.

AO-SLO Imaging

After pupil dilation, the RNF bundles were scanned using a custom-built, confocal AO-SLO system,[26] as described previously.[24,25] In particular, RNF bundles were imaged near the edge of the optic disc, along the temporal half of a circle at approximately 1.7 mm from the disc center, and if time permitted along a vertical line through the fovea. (The vertical imaging was a secondary measure as the RNF bundle thinning was less distinct in this region compared to the circumpapillary region where RNF bundles are thicker before damage.) The images were captured using 1.5° × 1.5° and 1.0° × 1.0° fields of view for the disc and macula, respectively. The retinal depth at which each patient was imaged was determined by adjusting focus. In particular, to ensure the innermost retinal nerve fiber layer (RNFL) surface was imaged for each subject, the adaptive optics (AO) focus was started just above the RNFL (i.e., at the vitreous) and then slowly shifted toward the surface of the RNFL.

Each image was the average of a sequence of frames with the highest signal-to-noise ratio. These images were montaged manually and coregistered with fundus photographs. Images from different scan dates also were aligned with the same fundus photograph using blood vessels as landmarks.

Results

Progress of the Edge of Deep Defects Near Fixation as Seen on AO-SLO

Figure 3A shows the montage of the AO-SLO images of patient P3OD obtained during the first (left) and last (right) AO-SLO visits. Figures 3B and 3E show an enlarged image of the region within the red and green squares in Figure 3A, and Figures 3C and 3D show the images for the same region obtained on the second and third visits. On the first visit, there is a region largely devoid of RNF bundles; the yellow lines indicate the approximate superior (solid) and inferior (dashed) borders of this region. To help visualize the changes over time, corresponding regions are indicated in Figures 3C to 3E. The red dots indicate blood vessel locations, the yellow double arrows show the width of the region with largely missing RNF bundles at two locations on the first visit, and the red arrows show the same location in Figures 3B to 3E.

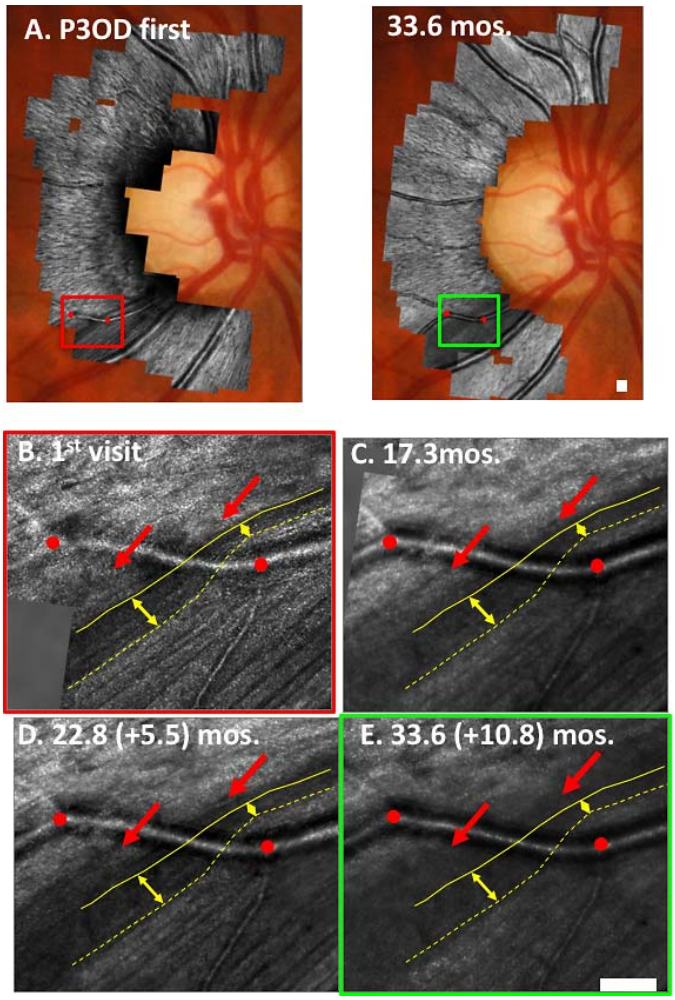

Figure 3. (A) Montage of the peripapillary AO-SLO images superimposed upon the fundus photograph of P3OD for the first (*left*) and last (*right*) visits. The regions within the *red* and *green rectangles* are expanded in (B) and (E), respectively. (C, D) The same region obtained during the second and third visits, which were 17.3 (C) and 22.8 (D) months after the first. The *red dots* indicate the same blood vessel locations in all Figures. The *yellow lines* and *arrows* are located in the same locations in (B–E) and show the borders and widths of the region without RNF bundles at the first visit (B). The *red arrows* also are in the same locations in (B–E) and indicate a region in which there appears to be progression of damage. *Scale bars*: ([A], *lower right*) is 100 μm and applies to both parts of (A); ([E], *lower right*) is 100 μm and applies to (B–E).

There appears to be progression of the RNF bundle loss during the 17.3 months between the first (Fig. 3B) and second (Fig. 3C) visits and during the 10.8 months between the third (Fig. 3D) and fourth (Fig. 3E) visits. The abnormal region (red arrows)

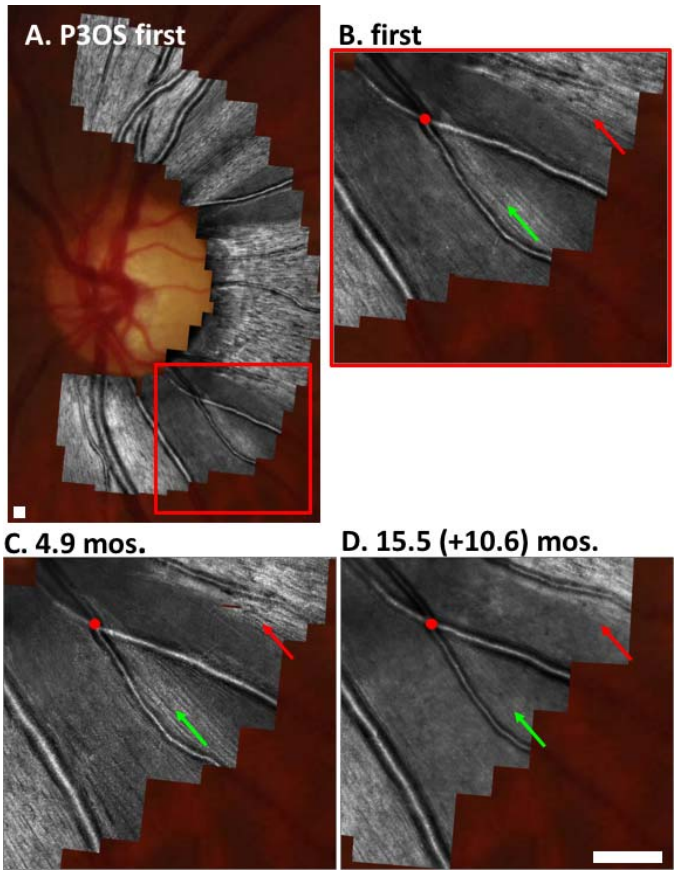

Figure 4. (A) Montage of the peripapillary AO-SLO images superimposed upon the fundus photograph of patient P3OS for the first visit. The region within the *red rectangle* is expanded in (B). (C, D) The same region obtained during the second and third visits, which were 4.9 (C) and 15.5 (D) months after the first. The *red dot* indicates the same blood vessel location in all Figures. The *red arrows* are in the same locations in (B–D) and indicate a region in which there appears to be progression of damage. The *green arrows* are in the same locations in (B–D) and indicate a region in which the RNF bundles lose contrast over time. *Scale bars*: ([A], *lower left*) 100 μm; ([D], *lower right*) 100 μm and applies to (B–D).

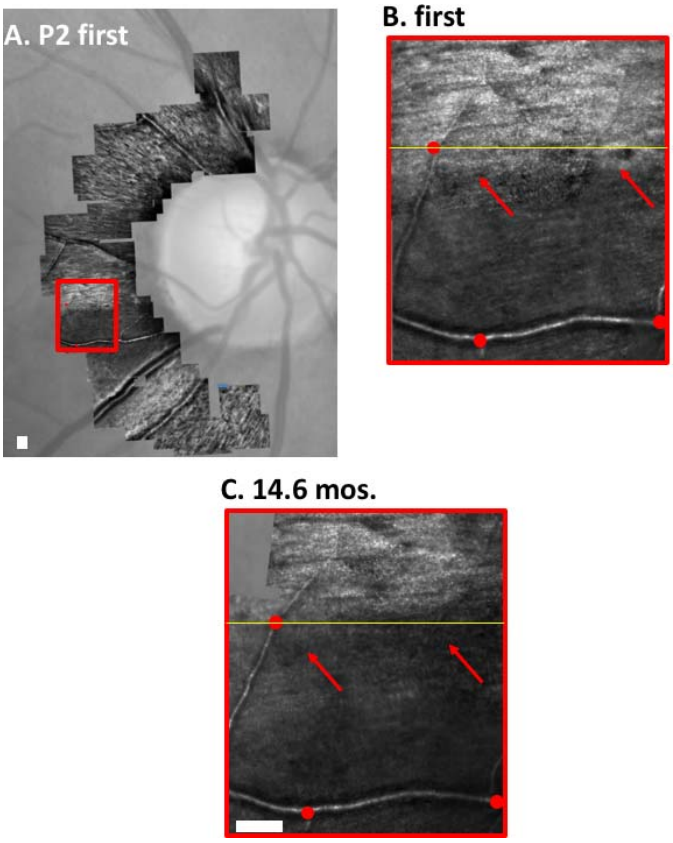

Figure 5. (A) Montage of the peripapillary AO-SLO images superimposed upon the fundus photograph of patient P2 for the first visit. The regions within the *red rectangle* is expanded in (B). (C) The same region obtained during the second visit, which was 14.6 (C) months after the first. The *red dots* indicate the same blood vessel location in all Figures. The *red arrows* are in the same locations in (B) and (C), and indicate a region in which there appears to be progression of damage. The *yellow horizontal lines* are in the same location in (B) and (C) and provide a reference for ease of comparing affected zones. *Scale bars*: ([A], *lower left*) 100 μm; ([C], *lower left*) 100 μm and applies to (B) and (C).

above the solid yellow line becomes larger over time. Notice that there appears to be little change during the 5.5 months between the second (Fig. 3C) and third (Fig. 3D) visits.

Three of the remaining five eyes (patient P3OS, Fig. 4; patient P2, Fig. 5; patient P1, Fig. 6) showed suggestions of progression of the edge between regions of missing bundle and largely present bundles in the same inferior-temporal region of the disc. The red arrows in Figures 4 to 6 show locations with an apparent loss of RNF bundles over time. That is, in each eye there are RNF bundles near the tip of the red arrow at the first visit and these bundles are less apparent over time.

In one of the two remaining eyes (patient P5) the presence of an epiretinal membrane (ERM) made it difficult to follow changes in the inferior temporal region as seen in Figure 7. In the other (patient P6, Fig. 8), the border between a clearly seen bundle (yellow arrows) appears to remain the same after 27.4 months.

Progressive Loss of Contrast of RNF Bundles within Defects Near Fixation as Seen on AO-SLO

In patient P6 (Fig. 8), the bundles in the region of the green arrows become less distinct (less contrast)

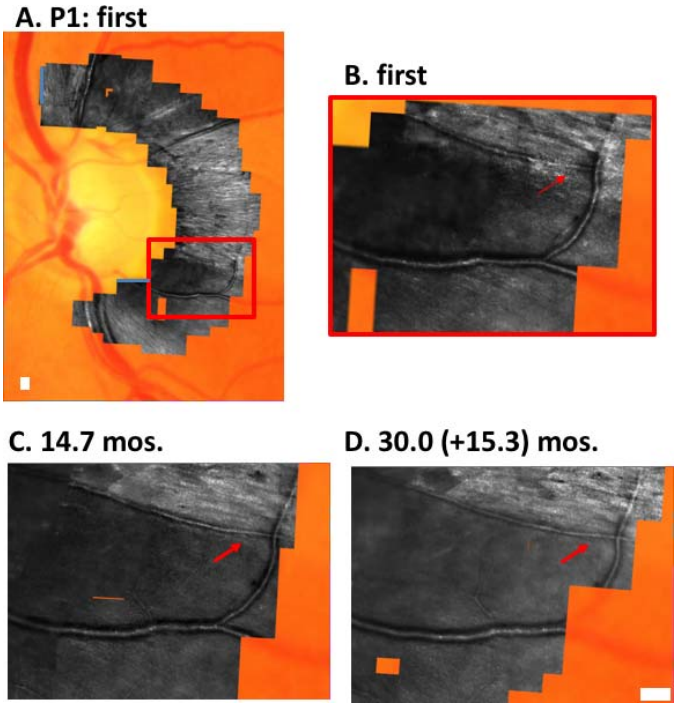

Figure 6. (A) Montage of the peripapillary AO-SLO images superimposed upon the fundus photograph of patient P1 for the first visit. The regions within the *red rectangle* is expanded in (B). (C, D) The same region obtained during the second and third visits, which were 14.7 (C) and 30.0 (D) months after the first. The *red arrows* are in the same locations in (B–D) and indicate a region in which there appears to be progression of damage. *Scale bars*: ([A], *lower left*) 100 μm; ([D], *lower right*) 100 μm and applies to (B–D).

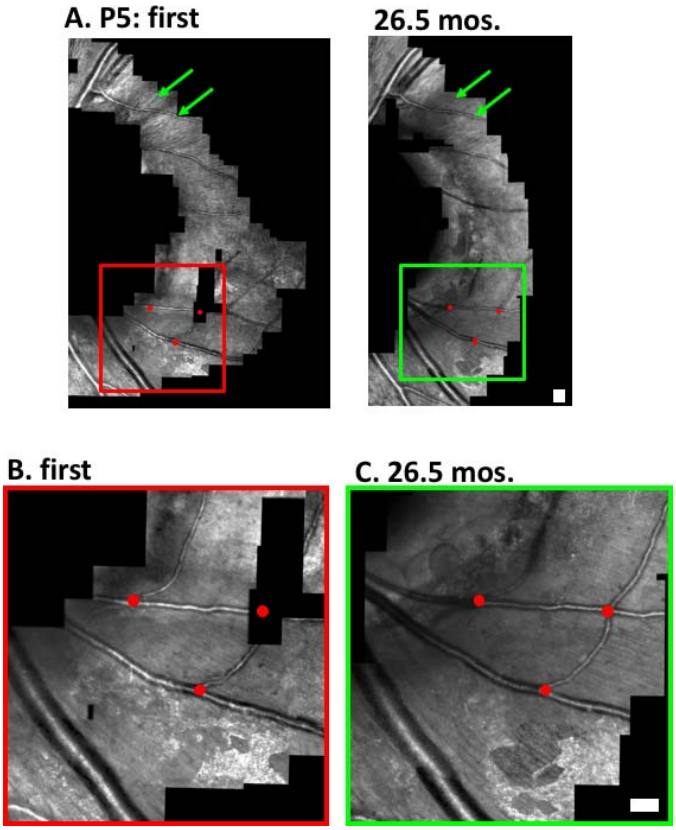

Figure 7. (A) Montage of the peripapillary AO-SLO images of P5 for the first (*left*) and last (*right*) visits. The regions within the *red* and *green rectangles* are expanded in (B) and (C), respectively. The *red dots* indicate the same blood vessel location in all panels. The *green arrows* in (A) are in the same locations and indicate a region in which there appears to be progression of damage. *Scale bars*: ([A], *lower right*) 100 μm and applies to both parts of [A]; ([C], *lower right*) is 100 μm and applies to (B) and (C).

between the first and last images. In addition to patient P6, patient P3OS (Fig. 4) also showed evidence of a loss of contrast in the remaining RNF bundles. For example, compare the regions near the green arrows at the first and last visits. The bundles lose contrast and become harder to discern over the 15.5-month period. On the other hand, there appears to be little change between the images from the first and second visits, which were only 4.9 months apart.

Superior Disc/Lower VF Defects

Two eyes (P1 and P3OS) also had deep arcuate defects near fixation in the inferior 10-2 VF (Figs. 1, 2). In both cases, the edge of the high contrast bundles changed/moved over time as seen by the red arrows in Figure 9. In addition, in both eyes there was an indication of a change in contrast of the bundles in the affected area (green arrows).

Further, note in Figure 7A there also is a region (green arrows) in the superior disc with a clear change in contrast between the two test dates. This disc region is outside the area associated with the 10-2 VF. Progression was seen in the associated region on 24-2 VF and OCT scans (not shown).

Discussion

Our primary purpose was to understand the nature of glaucoma progression in terms of RNF loss as seen with AO-SLO. We identified two aspects of progression of deep defects near fixation. First, in four of the six eyes, the edge of the region with healthy-appearing RNF bundles moved in the direction of fixation. That is, we have evidence of subtle progression of damage toward fixation within 10.6 (patient P3OS) to 14.7 (patient P1) months in these four eyes. In addition, within the abnormal regions there also was a suggestion of a loss of contrast of the remaining bundles over a similar time period.

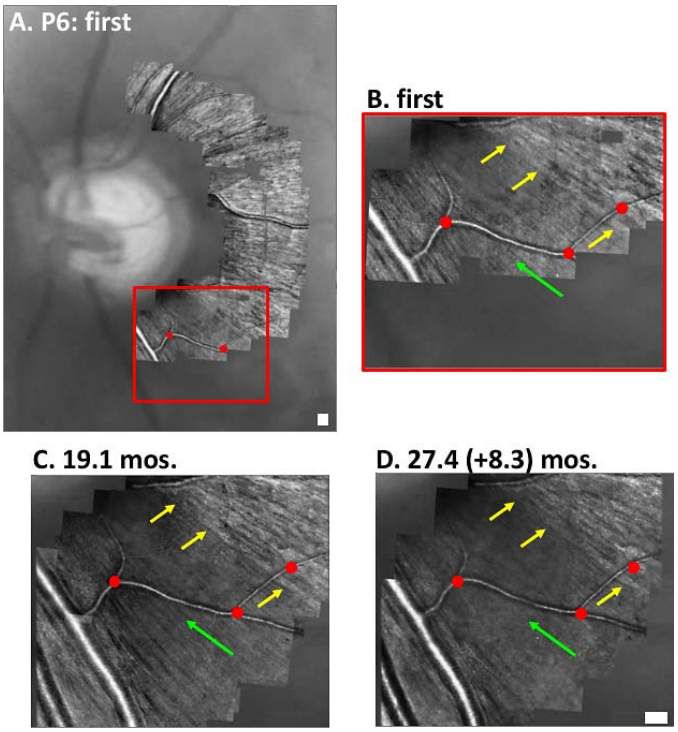

Figure 8. (A) Montage of the peripapillary AO-SLO images superimposed upon the fundus photograph of P6 for the first visit. The region within the *red rectangle* is expanded in (B). (C, D) The same region obtained during the second and third visits, which were 19.1 (C) and 27.4 (D) months after the first. The *red dots* indicate the same blood vessel location in all Figures. The *yellow arrows* are in the same locations in (B–D) and indicate the edge of a defect that does not appear to change over time. The *green arrows* also are in the same location in (B–D) and indicate a region in which the remaining RNF bundles appear to lose contrast. *Scale bars*: ([A], *lower left*) 100 μm; ([D], *lower right*) 100 μm and applies to (B–D).

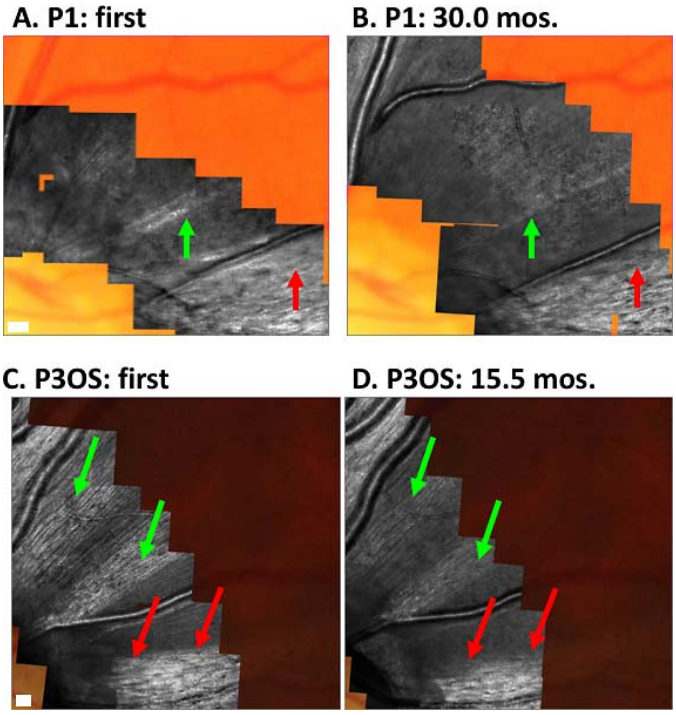

Figure 9. The superior temporal portion of montage of the peripapillary AO-SLO images superimposed upon the fundus photograph of P1 for the first (A) and last (B) visits and of P3OS for the first (C) and last (D) visits. *Green arrows* indicate a region in which the remaining RNF bundles appear to lose contrast, and *red arrows* a region of the edge of the defect that appears to lose RNF bundles, over time. *Scale bar*: *lower left* of all Figures is 100 μm.

Both types of change seen on AO-SLO are consistent with what we know about glaucoma progression. The loss of RNF bundles at the edge of the defect very likely is associated with the increase in the area of damage seen on OCT scans and VFs. However, we must exercise caution in interpreting the loss of contrast of bundles within the defect, as contrast can be influenced by several factors, including the plane of focus and variations in the brightness and contrast of AO-SLO images. Irrespective of these, it is likely that at least some of this decrease of contrast is due to a loss of RNF axons, as we know that a thinning on the RNFL seen on OCT scans can be associated with a lower contrast seen on AO-SLO images.[25] This is illustrated for patient P3OD in Figure 10, where the image on the right is a portion of the AO-SLO image from Figure 3A (left), and the image on the left is a portion of a circumpapillary OCT circle scan of the same region from a previous study.[25] The violet lines show corresponding locations of two blood vessels, which border the region of lower contrast on the AO-SLO image and thinner RNFL on the OCT scan.

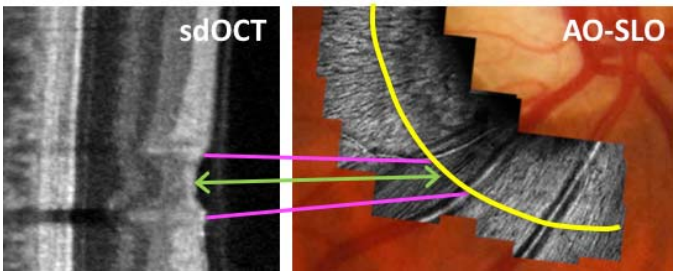

Figure 10. A comparison of the circumpapillary OCT circle scan (*left*) and AO-SLO (*right*) images for the same region of P3OD. The *yellow semicircle* indicates the locus of the OCT scan; the *purple lines* indicate the alignment of blood vessels; and the *green arrows* the same region showing thinning of the RNFL on OCT (*left*) and loss of contrast on AO-SLO (*right*).

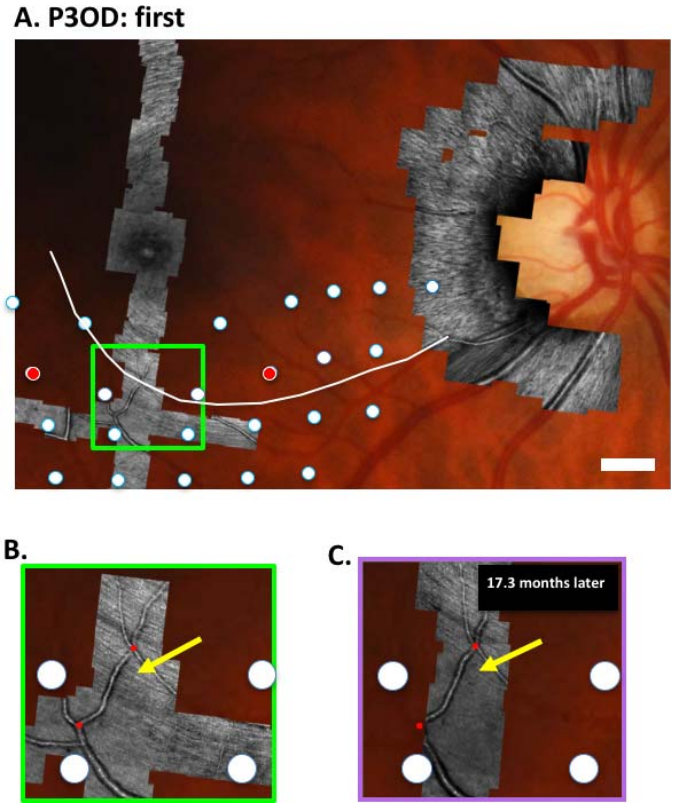

Figure 11. (A) Montage of the peripapillary AO-SLO images superimposed upon the fundus photograph of P3OD from the first visit (as in Fig. 3A) along with the montage of the AO-SLO images obtained along the vertical meridian. The *white dots* indicate the estimated locations of 10-2 visual field points in the region of interest, while the *red dots* are the two locations shared by the 10-2 and 24-2 VFs. The locations of the VF points have been adjusted to take into consideration the displacement of the ganglion cells near the fovea. The *white line* is the approximation of the course the RNF axons take above the edge of the defect. (B) An enlarged image of the region within the *green rectangle*. (C) The same region 17.3 months later. The *yellow arrows* in (B) and (C) are in the same location. *Scale bar*: *lower right* of (A) 500 μm.

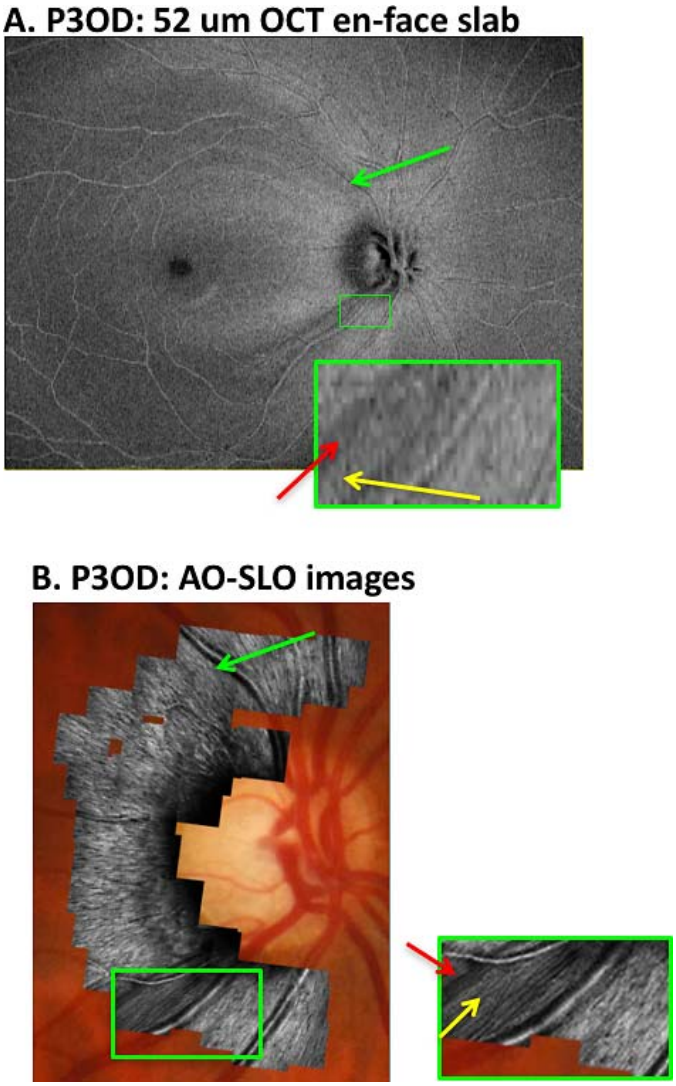

Figure 12. (A) An en face OCT image obtained for P3OD by averaging the reflectance intensity of a region (slab) between the ILM and 52 μm below the ILM.[28] (B) Montage of the peripapillary AO-SLO images superimposed upon the fundus photograph of patient P3OD for the first visit (as in Fig. 3A). The *green rectangles* and *arrows* in both Figures are the same regions of the superior temporal (*arrows*) and inferior temporal (*rectangles*) disc. The *yellow* and *red arrows* show regions of missing (*red*) RNF bundles and bundles of low contrast (*yellow*).

Comparison of AO-SLO Images to VF and OCT

These subtle changes at the edge of the defects seen on AO-SLO will be hard to see on traditional VFs, even with the 10-2 test pattern. To illustrate this point, Figure 11A shows the circumpapillary AO-SLO images from Figure 3A and the AO-SLO images along the vertical meridian taken in the same session.[24] The locations of the 10-2 VF points nearest the defect are indicated by the white dots, while the two red locations are shared by the 10-2 and 24-2 VFs. The locations of all VF points were adjusted for average displacement of the RGC near the fovea, as described previously.[8,27] The dots also are drawn to match approximately the size of the VF test light. The white line shows the approximate route of the RNF bundles just superior to the edge of the defect, which is just above the affected region. Notice with AO-SLO, we see loss at the level of single RNF bundles. This can be seen best on the enlarged image in Figure 3B. Figure 3C shows this same region 17.3 months later. Notice that the region at, and just below, the

yellow arrows show clear RNF bundles at the first visit (Fig. 3B), but little or no indication of bundles 17.3 months later. Notice also that there are a number of such bundles between the points of the 10-2 VF. Thus, the 10-2 will not be able to resolve some of the details seen on AO-SLO.

OCT also has better spatial resolution than the 10-2 VF. However, the lateral/transverse resolution of the OCT is poorer than that of AO-SLO, so that details in that direction will not, in general, be seen as well. In any case, a good way to visualize the local variations in RNF thickness and intensity on OCT scans is with en face images obtained by averaging the OCT reflectance intensity in a slab of constant width below the inner limiting membrane (ILM).[28] Figure 12A shows the en face image obtained for patient P3OD from a swept-source OCT scan obtained on the same day as the AO-SLO images in Figure 3A, which are reproduced in Figure 12B. The en face image in Figure 12A was based upon a nominal 9 × 12 mm scan with 256 b-scans, each with 512 a-scans.[28] When comparing the same location in the inferior temporal region of the disc (green rectangle), the same pattern of RNF loss is apparent on the OCT en face (Fig. 12A) and AO-SLO (Fig. 12B) images. However, the details are seen better on the AO-SLO image. While the resolution of these details can be improved by increasing the density of the a- and b-scans, we expect that it will not equal that obtained with high quality AO-SLO images.

On the other hand, there is a pattern of arcuate losses in the superior retina of this same eye that arguably is easier to see on the OCT en face image. Compare the regions indicated by the green arrow on the en face (Fig. 12A) and AO-SLO (Fig. 12B) images. It is easier to visualize an abnormal region on the complete en face image in Figure 12A. To be fair, this en face image has the advantage of a wide view that helps to identify the abnormal regions. Thus, a proper comparison requires a larger montage of AO-SLO images, which would take considerable time to obtain. In any case, it not surprising that a decrease in thickness may be easier to see on OCT given it has better axial resolution than does AO-SLO.

Clinical Implications

Our secondary purpose was to explore the use of AO-SLO imaging in detecting progression in the clinic or clinical trials. As previously noted,[24] it has a limited role with current technology. First, patients cannot have dry eyes, high refractive errors, significant cataracts, or ERM. Further, the circumpapillary images take over 45 minutes to obtain and many hours to analyze. However, Chen et al.[24] speculated that AO-SLO imaging of a restricted portion of the disc might be of use in small clinical trials designed to monitor progression. Our results suggested that it may be of value when it is important to detect very early changes in deep arcuate defects. In particular, no other current technology allows us to see the loss of individual RNF bundles with the same detail. On the other hand, we would add to the caveats above that subtle thinning might be difficult to detect with AO-SLO and that OCT measures, including combined AO and OCT,[19] might actually be superior for detecting these changes; they will certainly be quicker and easier to obtain and analyze.

Limitations

This study has two main limitations. First, the sample size is small. Second, the analysis is qualitative. While the movement of the edge of the defect should, in principle, be possible to quantify, the detection of contrast is more complicated. In any case, even if contrast changes due to RNFL thinning are reliably distinguished from other sources of contrast variations, it is unlikely that AO-SLO will be superior to OCT for detecting RNFL thinning for reasons mentioned above.

Conclusions

Progression of damage of deep arcuate defects near fixation is manifested on AO-SLO images in two ways. Over a period of approximately 1 year, there is a loss of individual RNF bundles at the edge of these defects. In addition, bundles remaining in the region of the defect lose contrast. These subtle changes will not be detectable on a 10-2 VF, and may or may not be seen with OCT en face imaging. On the other hand, subtle thinning of the RNFL is not easy to see with current AO-SLO technology and probably is better followed with OCT.

Acknowledgements

Supported by the National Eye Institute (NEI) of the National Institutes of Health (Bethesda, MD) under award numbers R01EY02115, R01EY025231, and U01EY025477, as well as the Joseph and Marilyn Rosen Research Fund of the New York Glaucoma

Research Institute, the Glaucoma Research Foundation Catalyst for a Cure Initiative, the Marrus Family Foundation, the Wise Family Foundation, the Lowenstein Foundation, the New York Eye and Ear Chairman's Research Fund, and the Violett Fund, Milbank Foundation.

Disclosure: **D.C. Hood**, None; **D. Lee**, None; **R. Jarukasetphon**, None; **J. Nunez**, None; **M.A. Mavrommatis**, None; **R.B. Rosen**, None; **R. Ritch**, None; **A. Dubra**, None; **T.Y.P. Chui**, None

References

1. Aulhorn E, Harms M. Early visual field defects in glaucoma. In: Leydhecker W, ed. *Glaucoma, Tutzing Symposium*. Basel: Karger; 1967:151–156.
2. Drance SM. The early field defects in glaucoma. *Invest Ophthalmol Vis Sci*. 1969;8:84–91.
3. Anctil JL, Anderson DR. Early foveal involvement and generalized depression of the visual field in glaucoma. *Arch Ophthalmol*. 1984;102:363–370.
4. Heijl A, Lundqvist L. The frequency distribution of earliest glaucomatous visual field defects documented by automatic perimetry. *Acta Ophthalmol (Copenh)*. 1984;62:658–664.
5. Langerhorst CT, Carenini LL, Bakker D, De Bie-Raakman MAC. Measurements for description of very early glaucomatous field defects. In: Wall M, Heijl A, eds. *Perimetry Update 1996/1997*. New York: Kugler Publications; 1997:67–73.
6. Hood DC, Raza AS, de Moraes CG, et al. Glaucomatous damage of the macula. *Prog Retin Eye Res*. 2013;32:1–21.
7. Schiefer U, Papageorgiou E, Sample PA, et al. Spatial pattern of glaucomatous visual field loss obtained with regionally condensed stimulus arrangements. *Invest Ophthalmol Vis Sci*. 2010;51:5685–5689.
8. Hood DC, Raza AS, de Moraes CG, et al. Initial arcuate defects within the central 10 degrees in glaucoma. *Invest Ophthalmol Vis Sci*. 2011;52:940–946.
9. Park, SC. Kung Y, Su D et al. Parafoveal scotoma progression in glaucoma: Humphrey 10-2 versus 24-2 visual field analysis. *Ophthalmology*. 2013;120:1546–1550.
10. Traynis I, de Moraes CG, Raza AS, et al. The prevalence and nature of early glaucomatous defects in the central 10° of the visual field. *JAMA Ophthalmol*. 2014;132:291–297.
11. Hangai M, Ikeda HO, Akagi T, Yoshimura N. Paracentral scotoma in glaucoma detected by 10-2 but not by 24-2 perimetry. *Jpn J Ophthalmol*. 2014;58:188–96.
12. Grillo LM, Wang DL, Ramachandran R, et al. The 24-2 visual field test misses central macular damage confirmed by the 10-2 visual field test and optical coherence tomography. *Trans Vis Sci Tech*. 2016;5:15.
13. Park HY, Hwang BE, Shin HY, Park CK. Clinical cues to predict the presence of perifoveal scotoma on Humphrey 10-2 visual field using a Humphrey Visual Field. *Am J Ophthalmol*. 2016;161:150–159.
14. Sullivan-Mee M, Tran MTK, Pensyl D, et al. Prevalence, features and severity of glaucomatous visual field loss measured with the 10-2 achromatic threshold visual field test. *Am J Ophthalmol*. 2016;168:41–50.
15. Hood DC, Raza AS, de Moraes CG, et al. The nature of macular damage in glaucoma as revealed by averaging optical coherence tomography data. *Trans Vis Sci Technol*. 2012;1:1–15.
16. Hood DC, Slobodnick A, Raza AS, et al. Early glaucoma involves both deep local, and shallow widespread, retinal nerve fiber damage of the macular region. *Invest Ophthalmol Vis Sci*. 2014;55:632–649.
17. Ramulu PY, West SK, Munoz B, et al. Driving cessation and driving limitation in glaucoma: the Salisbury Eye Evaluation Project. *Ophthalmology*. 2009;116:1846–1853.
18. Ramulu PY, West SK, Munoz B, et al. Glaucoma and reading speed: the Salisbury Eye Evaluation project. *Arch Ophthalmol*. 2009;127:82–87.
19. Kocaoglu OP, Cense B, Jonnal RS, et al. Imaging retinal nerve fiber bundles using optical coherence tomography with adaptive optics. *Vis Res*. 2011;51:1835–1844.
20. Takayama K, Ooto S, Hangai M, et al. High resolution imaging of the retinal nerve fiber layer in normal eyes using adaptive optics scanning laser ophthalmoscopy. *PLoS One*. 2012;7:33158.
21. Takayama K, Ooto S, Hangai M, et al. High resolution imaging of retinal nerve fiber bundles in glaucoma using adaptive optics scanning laser ophthalmoscopy. *Am J Ophthalmol*. 2013;155:870–881.
22. Scoles D, Higgins BP, Cooper RF, et al. Microscopic inner retinal hyper-reflective pheno-

types in retinal and neurologic disease. *Invest Ophthalmol Vis Sci*. 2014;55:4015–4029.
23. Huang G, Gast TJ, Burns SA. In vivo adaptive optics imaging of the temporal raphe and its relationship to the optic disc and fovea in the human retina. *Invest Ophthalmol Vis Sci*. 2014;55: 5952–5961.
24. Chen MF, Chui TYP, Alhadeff P, et al. Adaptive optics imaging of healthy and abnormal regions of retinal nerve fiber layers. *Invest Ophthalmol Vis Sci*. 2015;56:674–681.
25. Hood DC, Chen MF, Lee D, et al. Confocal adaptive optics imaging of peripapillary nerve fiber bundles: implications for glaucomatous damage. *Transl Vis Sci Technol*. 2015;4):12.
26. Dubra A, Sulai Y. Reflective afocal broadband adaptive optics scanning ophthalmoscope. *Biomed Opt Express*. 2011;2:1757–1768.
27. Hood DC, Raza AS. Method for comparing visual field defects to local RNFL and RGC damage seen on frequency domain OCT in patients with glaucoma. *Biome. Op. Exp*. 2011;2: 1097–1105.
28. Hood DC, Fortune B, Mavrommatis MA, et al. Details of glaucomatous damage are better seen on OCT en face images than on OCT retinal nerve fiber layer thickness maps. *Invest Ophthalmol Vis Sci*. 2015;56:6208–6216.